# Beam-exposure dependence and mechanisms of photon-stimulated desorption from alkali fluorides

C. C. Parks and D. A. Shirley

*Materials and Molecular Research Division, Lawrence Berkeley Laboratory and Department of Chemistry,*
*University of California, Berkeley, California 94720*

G. Loubriel

*Sandia National Laboratories, Albuquerque, New Mexico 87108*

Photon-stimulated desorption experiments were performed on the (001) face of LiF for photon energies near the F(2s) and Li(1s) edges (from 37 to 72 eV). There are structures in the F$^+$ yield above the F(2s) edge which are absent in the Li$^+$ spectrum, differences in detail in the Li$^+$ and F$^+$ yields near the Li(1s) edge, and considerable broadening of the desorption yields as compared to the bulk photoabsorption spectrum. The first observation of a strong x-ray and visible beam-exposure dependence of ion yields from LiF and NaF is also presented. These results are discussed in terms of electronic and defect properties of alkali halides.

## I. INTRODUCTION

Photon-stimulated desorption (PSD) of ions from alkali halides occurs following ionization of core levels.[1-3] In the Auger decay mechanism of desorption,[4,5] ionization of surface-atom core levels is followed by an Auger decay process involving the loss of two or more electrons from the valence band. The resulting multihole final state may be repulsive, and surface alkali or halogen species may desorb as positive ions. Because both alkali and halogen ion desorption result from the repulsive states produced by the Auger decay, their yields should be almost identical functions of photon energy and should strongly resemble the photoabsorption spectrum. In fact, the Na$^+$ and F$^+$ yields from NaF are very similar to photoabsorption near the Na(1s) edge.[3] Ion and excited neutral desorption near the Li(1s) level of LiF have been studied previously, but without mass resolution.[1] In this paper we shall compare ion yields and photoabsorption in detail at the F(2s) and Li(1s) edges of LiF. Our intent is to test the applicability of the Auger decay model in the best-studied of the alkali fluorides.

We shall also describe a strong dependence of alkali and hydrogen ion yields from alkali fluorides on x-ray beam exposure. The H$^+$ yield from freshly cleaved LiF and NaF crystals grows with total x-ray-beam exposure. The Na$^+$ yield from NaF increases with intense polychromatic light but falls back to normal in the presence of visible light or monochromatic x rays. Ion yields from NaF behave as if a single surface photoabsorption event could create PSD-active H$^+$ sites or destroy PSD-active Na$^+$ sites over an area of $\sim 10^4$ lattice sites. We propose mechanisms to account for this behavior. For instance, we propose that a photon activates a hydrogen species in the bulk, which migrates to the surface and is desorbed as H$^+$ by a subsequent photon.

Experimental methods are described in Sec. II. In Sec. III the ion-desorption spectra and photoabsorption are compared at the F(2s) and Li(1s) edges. In Sec. IV, the beam-exposure measurements from the LiF and NaF crystals are described and discussed. Conclusions are summarized in Sec. V.

## II. EXPERIMENTAL

The experiments were performed on beam line III-1 at the Stanford Synchrotron Radiation Laboratory using a "grasshopper" monochromator with a 600-line/mm grating. Charging was minimized by coating the sides of the samples with graphite before insertion in the vacuum chamber. Optical-quality NaF and LiF single crystals were cleaved *in situ* along the (001) plane at a pressure of $5 \times 10^{-10}$ Torr. The linearly polarized synchrotron radiation was incident at 45° from the normal along the crystalline [10$\bar{1}$] direction, so that the sample normal bisected the angle defined by the photon propagation and polarization directions. The positive-ion- and "prompt"-photon yields were collected normal to the samples using a time-of-flight analyzer with a drift tube biased between $-1000$ and $-1500$ V. The prompt yield is a 2.6-nsec full width at half maximum (FWHM) peak occuring in coincidence with the synchrotron light pulse. The analyzer detects only positive ions and photons, and has negligible efficiency[6] for photons below 7 eV. A 1500-Å aluminum window was inserted in the beam for all spectra between 37 and 72 eV to reduce second- and higher-order light. The ion- and prompt-yield spectra were normalized to the incident-photon flux as measured by the electron yield from a graphite-coated grid. Absolute flux measurements performed subsequently[7,8] with a National Bureau of Standards photodiode were used to estimate yields as counts per photon and to estimate x-ray exposures. The zero-order beam used in the beam-exposure measurements consisted of both visible and x-ray light. As an approximate measure of relative x-ray flux, the total electron yield from gold from the zero-order beam was 1600 times that from 160-eV radiation; this value was used in estimating exposures. A 0.5-mW He/Ne laser (Spectra Physics model 155) was used to determine the effects of visible

light on ion yields. The laser is monochromatic at 632.8 nm (1.96 eV), but has contaminant discharge light (estimated to be less than 10 $\mu$W) in the blue and green.[9] No attempt was made to prevent light from entering the chamber through viewports. After the experiment, the crystals were removed and examined carefully; no obvious coloration was seen. (The electron-beam-damaged LiF crystal had been recleaved and could not be checked afterwards.) The sodium fluoride cleaves were excellent; the lithium fluoride cleaves had some lateral fracture lines.

## III. Li(1s) AND F(2s) ION-YIELD SPECTRA FROM LiF

In this section we shall compare $Li^+$, $F^+$, and $H^+$ ion yields to bulk photoabsorption of LiF near the Li(1s) and F(2s) edges and discuss our results in terms of the Auger decay mechanism. We shall also describe the effects of electron-beam exposures on the $H^+$ yield spectra.

The Auger decay model leads to several predictions. The following decay pathways can result in desorption. After Li(1s) photoionization, the Li(1s) core hole may decay by an interatomic Auger process to produce a positive fluorine ion,

$$Li^{2+}+F^-\rightarrow Li^++F^++e^- \ . \tag{1}$$
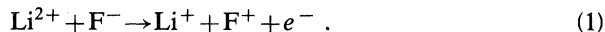
The resulting electrostatic environments of both the $F^+$ ion and neighboring $Li^+$ ions are repulsive;[3] the $F^+$ ion itself or a neighboring $Li^+$ ion can therefore desorb exothermally. The dominant species of hydrogen present in alkali halides[10,11] are interstitial hydrogen atoms ($H^0$), $H^-$ in halogen vacancies, and interstitial $H_2$. A decay process similar to Eq. (1) can lead to $H^+$ desorption of hydrogen from $H^-$ or $H^0$ sites. For the $H^-$ site, for instance, the Li-bonded $H^-$ becomes positively charged and can be expelled from the lattice as $H^+$,

$$Li^{2+}+H^-\rightarrow Li^++H^++e^- \ . \tag{2}$$
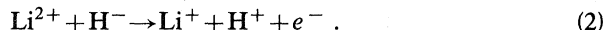
Following F(2s) excitation, an ordinary Auger decay,

$$F^0(2_s^1 2_p^6)\rightarrow F^++e^- \ , \tag{3}$$

may lead to $F^+$ and $Li^+$ desorption. Neighboring $H^-$ and $H^0$ species are spectators, and should not desorb as $H^+$. Therefore, we expect similar structures in $Li^+$ and $F^+$ desorption at the F(2s) and Li(1s) edges, and we expect these to resemble bulk photoabsorption. $H^+$ should have a threshold at the Li(1s) edge if Li-bonded hydrogen sites are present. We expect no $H^+$ yield threshold at the F(2s) edge if hydrogen is present only as $H^0$, $H^-$, and $H_2$.

In Fig. 1 we compare $Li^+$, $F^+$, $H^+$, and prompt yields from a LiF cleaved (001) surface to the photoabsorption spectrum of a thin evaporated film on an aluminium substrate, reported by Olson and Lynch.[12] The photon-energy resolution in the ion- and prompt-yield spectra was between 0.64 and 1.1 eV FWHM in the photon-energy range between 55 and 72 eV, while the resolution of the photoabsorption spectrum was 0.05 eV. Our LiF crystal was exposed to intense polychromatic (zero-order) light during alignment. Our monochromator was calibrated by matching the prompt peak with those of previous photoabsorption[12−17] and reflection[18−20] peaks at 61.9 eV.
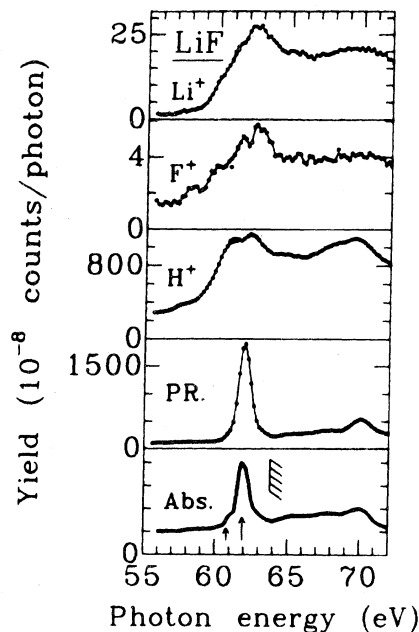


FIG. 1. Comparison of $Li^+$, $F^+$, $H^+$ and prompt (PR.) yields to bulk photoabsorption (Ref. 12). The Li(1s) photoionization threshold at 63.8 eV, the $Li^+$(1s→2s) exciton at 60.8 eV (short arrow), and the $Li^+$(1s→2p) exciton at 61.9 eV (long arrow), are indicated in the absorption spectrum. Curves are drawn through the data as a visual aid.

Photoabsorption near the Li(1s) threshold in LiF is well characterized. The shoulder at 60.8 eV and the prominent peak at 61.9 eV are assigned[21] to the $Li^+$(1s→2s) and $Li^+$(1s→2p) core excitons, respectively. The Li(1s) photoionization threshold[21] occurs at (63.8±0.4) eV. The "prompt"-photon-yield spectrum from our cleaved crystal in Fig. 1 agrees closely with the bulk photoabsorption spectrum, although it lacks the dipole-forbidden, phonon-assisted $Li^+$(1s→2s) exciton shoulder. We confirmed the lack of the shoulder at higher photon-energy resolution (0.2 eV at $h\nu$=60 eV). The nonspecular "prompt" signal had been interpreted previously as resonance fluorescence from the exciton and continuum states.[20] Because the prompt spectrum is bulk derived, it serves as a useful internal calibration for the surface-derived ion-yield spectra.

Contrary to our expectation that the ion-yield and photoabsorption spectra should be similar, the ion-yield spectra of Fig. 1 are considerably broader than the prompt or photoabsorption spectra. The three ion-yield spectra are quite similar, differing mainly in the relative intensities of some of the features. For instance, the "peak" at 69.5 eV is much larger in the $H^+$ spectrum than in the other spectra. All ion spectra exhibit a double-peaked structure between 60.9 and 62.8 eV. That structure changes slowly with time or beam exposure. These spectra (and those of Fig. 2) were taken several days after cleavage but differ only in minor details from spectra taken 6 h after cleavage. The $F^+$ spectrum has additional strucutres at 57.8 and 59.4 eV. If most of the ions desorbed from perfect (001) sites, we might expect the ion and photoabsorption spectra to be much more similar. The differences
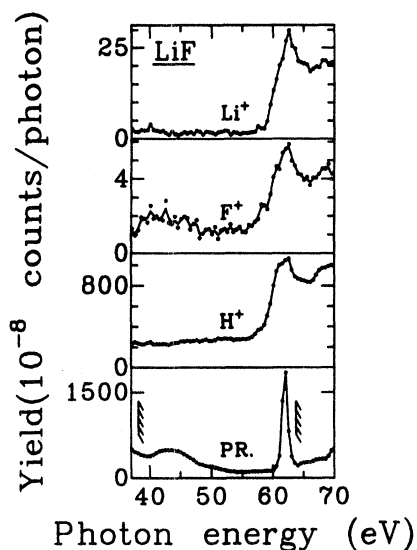
FIG. 2. Comparison of $Li^+$, $F^+$, and $H^+$ yields to prompt (PR.) yield. The F(2s) and Li(1s) binding energies at 38.2 and 63.8 eV, respectively, are indicated in the prompt spectrum. Curves are drawn through the data as a visual aid.



FIG. 3. $Li^+$, $H^+$, and prompt (PR.) yield spectra of the electron-beam-damaged surface. The crystal was exposed to a 1000-eV, 6-$\mu$A electron beam for 38 min. Curves are drawn through the data as a visual aid.

among the spectra (especially considering the broadening) are evidence that the desorption comes from complex minority sites or that the surface is very rough.

In Fig. 2 ion yields are compared with prompt yield between the F(2s) and Li(1s) photoionization thresholds[21] at (38.2±0.8) and (63.8±0.4) eV, respectively. A broad structure above the F(2s) photoionization threshold between 40 and 45 eV occurs in the prompt and in the $F^+$ yields, but is absent in $Li^+$ or $H^+$ desorption. The $Li^+$ ion yield increases by a factor of 20 at about 60 eV, while the $H^+$ and $F^+$ yields increase by only a factor of 4. Our $F^+$ spectrum, and the absolute electron-stimulated desorption (ESD) threshold[22] for $F^+$ at about 34 eV, are consistent with an Auger decay mechanism of $F^+$ desorption following F(2s) or Li(1s) photoabsorption. The Auger decay mechanism is *inconsistent* with the lack of a $Li^+$ threshold corresponding to the $F^+$ threshold near the F(2s) edge. The large jump in yield near the Li(1s) edge is further evidence that $Li^+$ desorption is weakly coupled to channels below the Li(1s) edge, but strongly coupled to photoabsorption of the Li(1s) core hole. Therefore, $F^+$ probably desorbs by the Auger decay mechanism, while $Li^+$ does not.

The threshold in $H^+$ yield at the Li(1s) edge is consistent with desorption from Li-bonded sites. The nature of these sites changes with beam exposure: the $H^+$ structure near 61.9 eV is somewhat different in Fig. 2 (for a crystal which had less beam exposure) than the structure in Fig. 1. As discussed previously, the lack of a threshold at the F(2s) edge is consistent with the Auger decay model: neutral or negatively charged hydrogen is not expected to desorb as $H^+$ following the F(2s 2p 2p) Auger decay. The $H^+$ yield is large below both the Li(1s) and F(2s) edges. Desorption below these edges could occur after single ionization of a Li-bonded hydrogen atom,

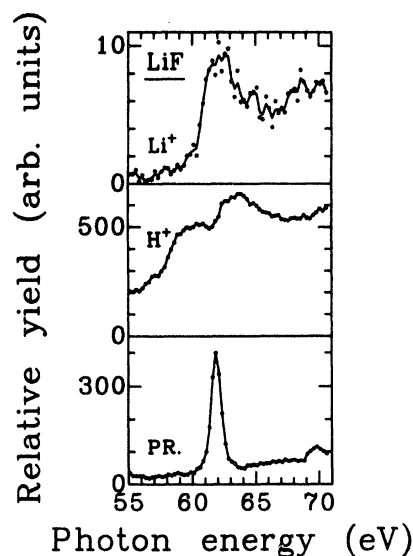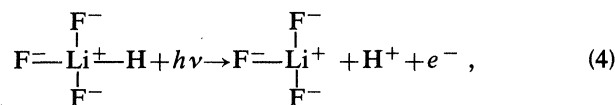$$ F\!-\!\overset{\displaystyle F^-}{\underset{\displaystyle F^-}{\underset{|}{\overset{|}{Li}}}}\!\!\pm\!\!H + h\nu \rightarrow F\!-\!\overset{\displaystyle F^-}{\underset{\displaystyle F^-}{\underset{|}{\overset{|}{Li}}}}{}^+ \;+H^+ + e^- \;, \qquad (4) $$

where the ionized hydrogen atom desorbs by repulsion from the $Li^+$ ion. Incidentally, the $H^+$ ions desorb with a higher kinetic energy than do $Li^+$ and $F^+$ ions at $h\nu = 62.8$ eV: The $^6Li^+$, $^7Li^+$, and $F^+$ times of flight scale as the square roots of the masses as expected, but the $H^+$ ions arrive sooner than expected.

We studied the effects of electron-beam damage on the ion yields. Electron-beam impact of alkali halides causes preferential desorption of halogen neutrals.[23,24] A surface-plasmon loss peak observed on a vacuum-cleaved LiF (100) surface using characteristic loss spectroscopy indicates that a thin surface layer of neutral lithium accumulates with electron-beam damage.[25] In Fig. 3 ion- and prompt-yield spectra are shown from a cleaved crystal exposed to a large (1000-eV, 6-$\mu$A, and 38-min) electron-beam exposure. Notice the sharper edge structure in the $Li^+$ spectrum as well as the dramatically changed $H^+$ spectrum. The prompt signal is unchanged as expected for a bulk process. The change in the $H^+$ spectrum must indicate formation of a new hydrogen surface species. Not surprisingly, all of the spectra differ from both Li metal[26] and lithium hydride[27,28] photoabsorption and fluorescence spectra.

## IV. BEAM-EXPOSURE DEPENDENCE OF ION YIELDS FROM NaF AND LiF

Time-dependent effects were observed in PSD ion yields from both NaF and LiF. To explore these effects we have carried out systematic studies of the dependence of ion yields on beam exposure. Several crystals were cleaved *in*
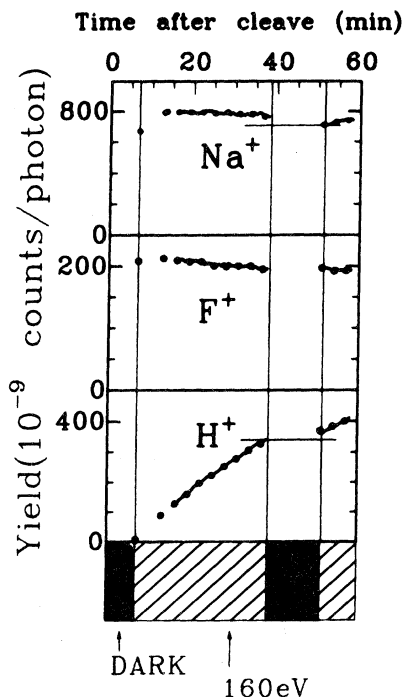
**Time after cleave (min)**



FIG. 4. $Na^+$, $F^+$, and $H^+$ yields at 160 eV vs time after cleavage. The following exposure sequence was performed: dark (0—7 min), 160 eV (7—38.5 min), dark (38.5—51.2 min), and 160 eV (51.2—59.2 min). For clarity one out of every five data points in enlarged.

*situ* and were subjected to sequential irradiation by soft x rays, zero-order light, and visible light. The results are presented below, in the spirit of reporting a survey of interesting phenomena. In general we cannot give unique explanations of these phenomena, but our observations set limits on the range of possible explanations, and plausible candidate mechanisms are hypothesized.

In Fig. 4 we plot ion yields from NaF in the first hour after cleavage. Monochromatic radiation (160 eV) was first allowed to strike the crystal 7 min after cleavage (subsequent times denote time elapsed after cleavage). The 160-eV photon energy was selected as the photon energy of maximum flux from the monochromator. This energy exceeds all but the $K$-shell binding energies of $Na^+$ and $F^+$ in NaF. The mass spectrum at 7 min showed weak (a few percent) peaks at masses corresponding to $NaF^+$ and $Na_2F^+$ as well as the $H^+$, $F^+$, and $H^+$ ion yields plotted in Fig. 4. The beam was shuttered at 38.5 min, and unshuttered again at 51.2 min. The 160-eV radiation flux[7,8] was approximately $10^{11}$ photons/(sec cm$^2$). The mean penetration depth is approximately 1000 Å, as estimated from atomic cross-section data.[29,30]

Two important conclusions emerge from Fig. 4. First, variations in $Na^+$ and $F^+$ yields with beam exposure are easily observable. These variations of $\sim 10\%$ are too large, relative to the cumulative surface depletion through desorption ($\leq 10^{-5}$ monolayers/min, an absolute upper bound based on assuming unity desorption of neutrals or ions per surface photoionization), to be attributable to gross changes in surface composition. Other explanations

must be sought.

Second, the $H^+$ yield is clearly radiation induced. It is also very large after sufficient exposure. Thus hydrogen-containing species must be both *created* by monochromatic (160-eV) radiation and *readily desorbed* by it, in two separate events. A plausible (but by no means unique) mechanism would involve a hydrogen species in the irradiated region of the bulk (about the first 1000 Å) being activated by irradiation, migrating to the surface and becoming trapped, and subsequently being ionized and desorbed by a second photon. For example, a $U$ center ($H^-$ in a halogen vacancy, a major form of hydrogen in alkali halides) could be converted to neutral hydrogen,[10]

$$U \rightarrow H^0 + F , \qquad (5)$$

leaving an F center behind. This conversion could occur directly by photoionization or indirectly through loss of a loosely bound electron on $H^-$ to a nearby radiation-induced positive site. If the neutral $H^0$ migrated to the surface on a timescale of minutes and became trapped in a surface site, facile desorption as $H^+$ would be expected, following photon absorption via an Auger decay mechanism. The timescale of minutes for migration of the slower $H^0$ species to the surface is inferred from the increase of $H^+$ yield following the dark period. This mechanism is consistent with the decreasing slope of the $H^+$
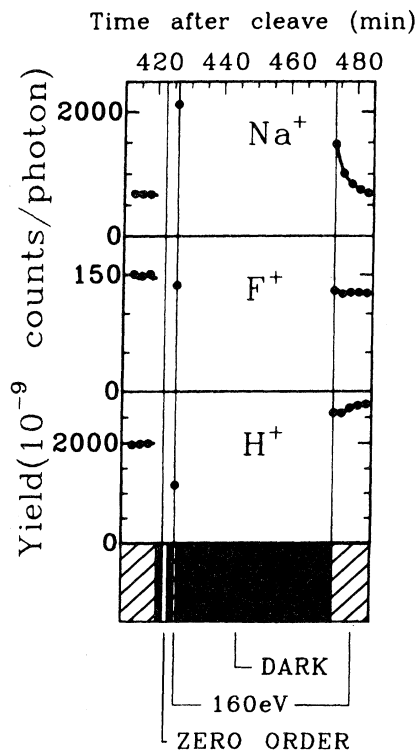
**Time after cleave (min)**



FIG. 5. $Na^+$, $F^+$, and $H^+$ yields at 160 eV vs time after cleavage. The following exposure sequence was performed: 160 eV (410—420.8 min), dark (420.8—422.6 min), zero order (422.6—424.3 min), dark (424.3—426.0 min), 160 eV (426.0—426.9 min), dark (426.9—473.4 min), and 160 eV (473.4—485 min). For clarity one out of every four data points is enlarged.

yield curve, which may imply saturation of active sites on the surface.

We tested the effects of large beam exposures by applying pulses of zero-order (intense polychromatic) light and measuring the subsequent ion yields versus time under irradiation with 160-eV light. In Fig. 5 results are shown of the following exposure sequence: 160-eV light, darkness interrupted by a zero-order pulse and a brief yield measurement at 160 eV, a long period of darkness, and further yield measurements at 160 eV. The zero-order exposure was composed of soft x rays (about $10^{16}$ photons/cm$^2$ as estimated using gold photoyield) and significant intensities of visible and ultraviolet light.

The initial decrease in $H^+$ yield followed by a slow rise to above the initial yield (seen in part in Fig. 5) is characteristic behavior following long zero-order exposures. When shorter (20-sec) zero-order exposures were applied, the initial decrease in $H^+$ yield did not occur, and the yield grew slowly from the initial value. According to the model described above, the initial decrease in yield would result from depletion of the surface active species (perhaps by desorption). The slow increase in $H^+$ yield would then occur as new PSD-active species diffused from the bulk to the surface.

The data in Fig. 5 establish several important facts concerning the $Na^+$ yield. First, the zero-order exposure causes an enhancement of the $Na^+$ yield. Second, the decay of the enhnaced $Na^+$ yield is induced by the 160-eV light. The strength of this effect is surprising because 5 min of exposure to 160-eV light results in about $10^{11}$ surface photoionizations per cm$^2$. Therefore, it would appear that each surface photoionization would have to eliminate PSD-active species over an area of $\sim 10^4$ lattice sites to account for the observed decay. This latter observation elminates a wide class of mechanisms from consideration in explaining the $Na^+$ yield enhancement.

Possible mechanisms for the enhanced $Na^+$ yield are restricted further by the observation that visible light also affects the $Na^+$ yield. We applied the following exposure sequence: 160-eV light, darkness, a zero-order exposure, darkness, and a long period of 160-eV light during which the crystal was exposed three times to a 1.96-eV (red) laser. Figure 6 shows the following results. First, the decay curve of the $Na^+$ yield became more gradual as the total exposure of the crystal accumulated. Second, illumination with the laser quenched the enhanced $Na^+$ yield. The laser had only a slight effect on the $Na^+$ yield if no zero-order light was applied previously.

The laser light interacts with the crystal by photoabsorption of a defect site. If the defect level lies close to the conduction band, photoconductivity can result. The laser photon energy is in a weakly absorbing region of the x-ray-irradiated crystal photoabsorption spectrum, far from the $F$ band (3.63 eV) and other color-center bands.[31,32] If we use the published absorbance (0.114) of a heavily x-ray-irradiated (1.4-mm-thick) NaF crystal[31] and our laser flux of $1.5 \times 10^{15}$ photons/sec, we estimate that an average of $10^8$ photons are absorbed per atomic layer per second. Although this estimate is crude, it demonstrates that each 1.96-eV surface photoabsorption would have to eliminate PSD-active sites over an area of $\sim 10^6$
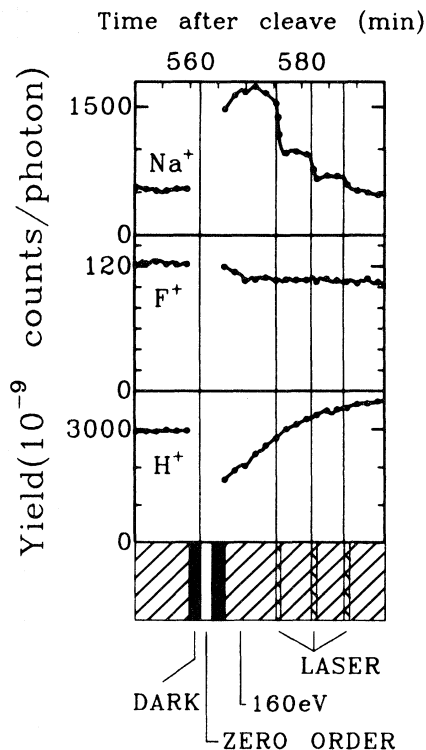
Time after cleave (min)



FIG. 6. $Na^+$, $F^+$, and $H^+$ yields at 160 eV vs time after cleavage. The following exposure sequence was performed: 160 eV (550—559.8 min), dark (559.8—561.8), zero order (561.8—563.9 min), dark (563.9—565.9 min), 160 eV (565.9—595 min). During the latter period, three laser exposures occurred: 575.4—576.2 min, 581.7—582.7 min, and 587.6—588.6 min. For clarity one out of every three data points is enlarged.

lattice sites to cause a substantial drop in yield.

A very speculative model consistent with some of the observations is the following. The band-gap component of the zero-order exposure produces mobile neutral sodium atoms which diffuse along the surface. The 160-eV photon creates a positively charged trap (such as $Na^{2+}$) which stops a neutral sodium atom passing by, ionizes the atom, and ejects the sodium species as a positive ion (which is detected). The essential feature of this mechanism is that the $Na^{2+}$ trap would effectively collect neutrals over a large area: A sodium atom with thermal kinetic energy travels several thousand Å in 1 nsec. This mechanism, while entirely speculative and dependent on the lifetime of the $Na^{2+}$ species, would explain both the enhancement of the $Na^+$ yield and the low flux necessary to quench the enhanced yield. However, it is uncertain how the laser affects the $Na^+$ yield in this mechanism.

Another speculative approach is to assume that the enhanced $Na^+$ yield is associated with the space charge generated by the zero-order light. The 160- and 1.96-eV radiation deplete this space charge by photoconductivity. Photoabsorption of many (10—100) layers would contribute to depletion of the space charge. The advantage of this approach is that it provides a framework for understanding the effects of the laser. The crucial difficulty here is that we have no mechanism for understanding why
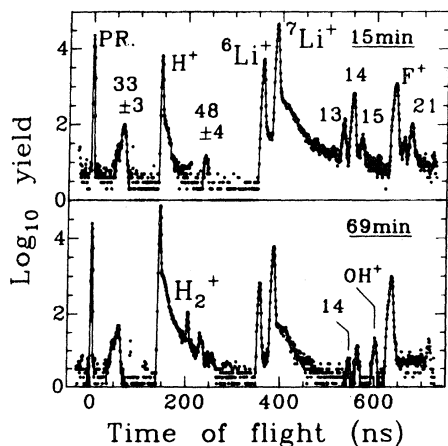
FIG. 7. Time-of-flight mass spectra from a freshly cleaved LiF crystal 15 min (upper panel) and 69 min (lower panel) after cleavage. The exposure sequence was dark and zero order (0—10 min), and 62.8 eV (10—69 min). The prompt yield is labeled "PR." As discussed in the text, probable mass assignments (in amu) are 13 ($^6$Li-$^7$Li$^+$), 14 ($^7$Li$_2^+$), 15 ($^7$Li$_2$H$^+$ or CH$_3^+$), 21 ($^7$Li$_3^+$), 33 ($^7$Li$_2$F$^+$), and 47 ($^7$Li$_4$F$^+$).
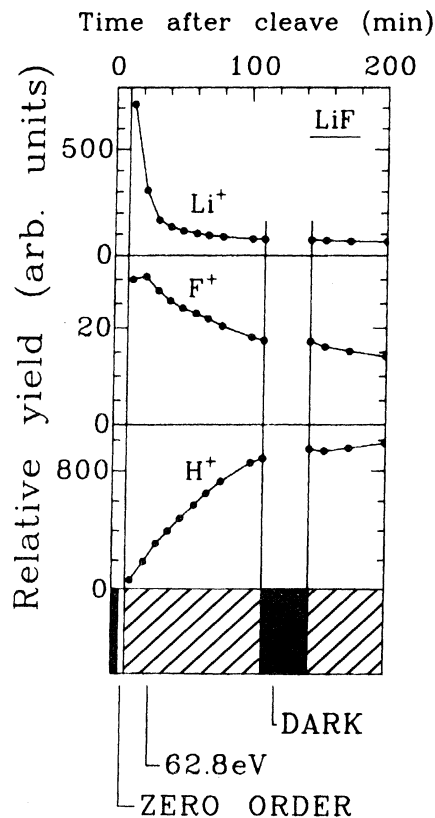


FIG. 8. Li$^+$, F$^+$, and H$^+$ yields at 62.8 eV vs time after cleavage. The following exposure sequence was performed: dark and zero order (0—10 min), 62.8 eV (10—114 min), dark (114—144 min), and 62.8 eV (144—200 min). Lines are drawn to connect the data points as a visual aid.

the Na$^+$ yield might be enhanced from the space-charged crystal.

In summary, the PSD ion yields from NaF were strongly affected by irradiation. Controlled experiments enabled us to characterize the effects and to narrow the range of possible explanations, but we were unable to develop a unique and complete model for the various observed phenomena.

Time-dependent ion yields were also observed from LiF. We exposed a LiF crystal to zero-order light shortly after cleavage and monitored ion yields under irradiation with monochromatic light (62.8 eV). The 62.8-eV energy was selected as being the photon energy giving the highest ion yields from LiF. Yields of species desorbing from the crystal 15 and 69 min after cleaveage are shown in Fig. 7. We assign several masses (13, 14, 21, 33, and 47 amu) to desorbing clusters rather than contaminant species because the ion yields decreased sharply with time, since we believe that our freshly cleaved surface was clean, and also because clusters have been observed to desorb previously from other alkali halides.[2] We can group these ion species according to time dependence. The ion yields of pure-lithium clusters ($^7$Li$_2^+$, $^6$Li-$^7$Li$^+$, and $^7$Li$_3^+$) decrease between 15 and 60 min by a factor of 100 or greater. In the second group, $^6$Li$^+$, $^7$Li$^+$, Li$_2$F$^+$, and F$^+$, ion yields decrease by factors ranging from 7 to 1.4. In the third group, H$^+$, Li$_4$F$^+$, and H$_2^+$, ion yields increase with time. In Fig. 8 we plot the time dependence of the H$^+$, $^7$Li$^+$, and F$^+$ ions. The time dependence of the H$^+$ and alkali ion yields is qualitatively similar in LiF and NaF.

Finally, we note that the effects of electron-beam exposures on ion yields from alkali halides in ESD have been characterized previously. Pian et al. reported that alkali-metal ion yields from NaCl increase with electron-beam exposure.[2] We confirmed this increase in the Na$^+$ yield from NaF in PSD following a large (1-$\mu$A, 70-eV, and 3-

min) electron-beam exposure, and we observed a large decrease in H$^+$ yield.

## V. CONCLUSIONS

We compared the ion-yield spectra near the F(2$s$) and Li(1$s$) thresholds with photoabsorption from LiF. Thresholds in F$^+$ yield were found at both the F(2$s$) and Li(1$s$) edges, as is expected in the Auger decay model. However, in contradiction with the expectations of the Auger decay model, the Li$^+$ yield had no threshold at the F(2$s$) edge. A threshold in H$^+$ yield from LiF occured at the Li(1$s$) edge, which is expected if Li-bonded hydrogen atoms or negative ions are present. We suggested that single ionization of Li-bonded hydrogen atoms is responsible for the H$^+$ yield at 37 eV below the F(2$s$) and Li(1$s$) edges. All the ion-yield spectra are considerably broadened in comparison to bulk photoabsorption at the Li(1$s$) edge, which is evidence that ion desorption comes from complex minority sites or that the surface is very rough.

Low-intensity x-ray and visible-light exposures affect ion yields from cleaved LiF and NaF surfaces. The H$^+$ yield from freshly cleaved LiF and NaF crystals grows as a function of total x-ray beam exposure. This growth in yield may result from conversion of hydrogen in the bulk (such as a $U$ center) to a mobile form which migrates to the surface and is desorbed by a subsequent photon.

Alkali-metal ion yields (Li$^+$, Li$_2^+$, Li$_3^+$, and Na$^+$) from LiF and NaF increase upon exposure to polychromatic light. The enhanced yields drop back to normal in the presence of monochromatic x rays or visible light (1.96 eV). While the mechanism for the enhanced alkali-metal ion yields is unknown, a major conclusion of our study is that defect properties are crucial in metal-ion desorption from these alkali halides.

## ACKNOWLEDGMENTS

[1]N. H. Tolk, M. M. Traum, J. S. Kraus, T. R. Pian, W. E. Collins, N. G. Stoffel, and G. Margaritondo, Phys. Rev. Lett. 49, 812 (1982).

[2]T. R. Pian, M. M. Traum, J. S. Kraus, N. H. Tolk, N. G. Stoffel, and G. Margaritondo, Surf. Sci. 128, 13 (1983).

[3]C. C. Parks, Z. Hussain, D. A. Shirley, M. L. Knotek, G. Loubriel, and R. A. Rosenberg, Phys. Rev. B 28, 4793 (1983).

[4]P. J. Feibelman and M. L. Knotek, Phys. Rev. B 18, 6531 (1978).

[5]M. L. Knotek, V. O. Jones, and V. Rehn, Phys. Rev. Lett. 43, 300 (1979).

[6]Galileo Electro-Optics Corp., Data sheet 4000B, September, 1980 (unpublished).

[7]D. Charleston (private communication).

[8]C. C. Parks, Ph.D. thesis, University of California—Berkeley 1983.

[9]R. Yazell (private communication).

[10]J. Schulman and W. Dale Compton, *Color Centers in Solids* (Pergamon, Oxford, 1962).

[11]P. D. Townsend and J. C. Kelly, *Colour Centres and Imperfections in Insulators and Semiconductors* (Crane, Russak, and Co., New York, 1973).

[12]C. G. Olson and D. W. Lynch, Solid State Commun. 31, 51 (1979).

[13]W. Gudat, C. Kunz, and H. Petersen, Phys. Rev. Lett. 32, 1370 (1974).

[14]A. A. Maiste, A. M.-É. Sarr, and M. A. Élango, Fiz. Tverd. Tela (Leningrad) 16, 1720 (1974) [Sov. Phys.—Solid State 16, 1118 (1974)].

[15]R. Haensel, C. Kunz, and B. Sonntag, Phys. Rev. Lett. 20, 262 (1968).

[16]A. P. Lukirskii, O. A. Ershov, T. M. Zimkina, and E. P. Savinov, Fiz. Tverd. Tela (Leningrad) 8, 1787 (1966) [Sov. Phys.—Solid State 8, 1422 (1966)].

[17]W. Gudat and C. Kunz, in *Proceedings of the IVth International Conference on Vacuum Ultraviolet Radiation Physics (Hamburg, 1974)*, edited by E. Koch, R. Haensel, and C. Kunz (Pergamon and Vieweg, Braunschweig, 1974), p. 392.

[18]N. Kosuch, G. Wiech, and A. Faessler, in *Proceedings of the IVth International Conference on Vacuum Ultraviolet Radiation Physics,* Ref. 17, p. 398.

[19]K. Tsutsumi, O. Aita, K. Ichikawa, M. Kamada, M. Okusawa, and T. Watanabe, in *Inner Shell and X-ray Physics of Atoms and Solids,* edited by D. J. Fabian, H. Kleinpoppen, and L. M. Watson (Plenum, New York, 1981), p. 775.

[20]O. Aita, K. Tsutsumi, K. Ichikawa, M. Kamada, M. Okusawa, H. Nakamura, and T. Watanabe, Phys. Rev. B 23, 5676 (1981).

[21]A. Zunger and A. J. Freeman, Phys. Rev. B 16, 2901 (1977).

[22]J. A. Schultz, P. T. Murray, R. Kumar, Hsin-Kuei Hu, and J. W. Rabalais, in *Proceedings of the First International Workshop on Desorption Induced by Electronic Transitions, Williamsburg, Virginia, 1982,* edited by N. H. Tolk, M. M. Traum, J. C. Tully, and T. E. Madey (Springer, Berlin, 1983), p. 191.

[23]P. D. Townsend, R. Browning, D. J. Garlant, J. C. Kelley, A. Mahjoobi, A. J. Michael, and M. Saidoh, Radiat. Eff. 30, 55 (1976).

[24]H. Overeijnder, M. Szymoński, A. Haring, A. E. de Vries, Radiat. Eff. 36, 63 (1978).

[25]L. S. Cota Araiza and B. D. Powell, Surf. Sci. 51, 504 (1975).

[26]T. A. Callcott, E. T. Arakawa, and D. L. Ederer, in *Extended Abstracts of the Vth International Conference on Vacuum Ultraviolet Radiation Physics, Montpellier, 1977,* edited by M. C. Castex, M. Pouey, and N. Pouey (CNRS, Meudon, 1977), Vol. 1, p. 275.

[27]A. A. Maiste, S. O. Cholakh, F. F. Gavrilov, and M. A. Élango, Fiz. Tverd. Tela (Leningrad) 16, 301 (1974) [Sov. Phys.—Solid State 16, 203 (1974)].

[28]T. Miki, M. Ikeya, Y. Kondo, and H. Kanzaki, Solid State Commun. 39, 647 (1981).

[29]I. M. Band, Yu. I. Kharitonov, and M. B. Trzhaskovskaya, At. Data Nucl. Data Tables 23, 443 (1979).

[30]G. V. Marr and J. B. West, At. Data Nucl. Data Tables 18, 497 (1976).

[31]K. Konrad and T. J. Neubert, J. Chem. Phys. 47, 4946 (1967).

[32]H. Blum, Phys. Rev. 128, 627 (1962).